The 11th Canadian Conference on Earthquake Engineering
Canadian Association for Earthquake Engineering

EFFECT OF IN-PLANE REVERSED CYCLIC LOADING ON THE OUT-OF-PLANE STABILITY OF REINFORCED MASONRY SHEAR WALLS

Brook R. Robazza
PhD Student, University of British Columbia, Canada
brook.robazza@civil.ubc.ca

Svetlana Brzev
Faculty, British Columbia Institute of Technology, Canada
sbrzev@bcit.ca

Tony Y. Yang
Assistant Professor, University of British Columbia, Canada
yang@civil.ubc.ca

Kenneth J. Elwood
Professor, University of Auckland, New Zealand
k.elwood@auckland.ac.nz

Donald L. Anderson
Emeritus Professor, University of British Columbia, Canada
dla@civil.ubc.ca

ABSTRACT: In Canada and other countries, reinforced masonry shear walls (RMSWs) often constitute the principal seismic force resisting system of masonry structures. During an earthquake, these walls face the combined effects of axial loading and in-plane overturning moments induced by lateral seismic forces. The combined actions may precipitate out-of-plane instability of the wall end zones at high levels of lateral drift when the longitudinal reinforcing bars in these regions experience numerous cycles of high tensile strain. To prevent this instability, the Canadian masonry design standard (CSA S304-14) stipulates stringent limits on the height-to-thickness (h/t) ratio of ductile RMSWs. The objectives of the current research are to evaluate the CSA S304-14 h/t limits and establish rational criteria for the out-of-plane stability of RMSWs. To accomplish this, five full-scale slender RMSW specimens with ductile detailing and varying height-to-length and h/t ratios, reinforcement amount and layout, axial stress level, and loading setup have been tested to date using a lateral in-plane reversed cyclic loading protocol until failure. The results indicate that h/t limits alone are insufficient for evaluating RMSW vulnerability to out-of-plane instability. A more robust and practical set of criteria may be established by setting limits on the axial tensile strain at the wall ends while taking into account vertical and lateral strain gradient effects, and considering possible occurrence of toe crushing or sliding mechanisms which would prevent development of out-of-plane instability.

1. Introduction

RMSWs are classified by the National Building Code of Canada 2010 (NBCC 2010) and CSA S304-14 based on their ability to dissipate energy during earthquake shaking. The wall classes are listed as "Conventional Masonry Shear Walls," "Moderately Ductile Shear Walls," or "Ductile Shear Walls" (MDSWs) with corresponding ductility-related force modification factors, R_d, of 1.5, 2.0, and 3.0 respectively (note that R_d = 1.0 denotes elastic seismic response). NBCC 2010 requires an R_d of 2.0 for all post-disaster buildings (e.g. police stations, fire halls, and pump stations), which therefore mandates the use of MDSWs, regardless of the location's seismicity. One of the CSA S304-14 seismic detailing requirements with very significant impact are the prescribed height/thickness (h/t) limits for ductile RMSWs. These limits have been

included to ensure stability of RMSWs under the combined effects of axial loads, in-plane seismic shear forces, and overturning moments, as shown in Fig. 1. High levels of lateral drift create large tensile strain demands at the wall's tension end zone. Reloading this end of the wall into compression may bring about out-of-plane displacements that may potentially precipitate instability and a severe reduction in the wall's performance. The h/t limits are derived from a formulation developed by Paulay and Priestley (Paulay and Priestley, 1993) which determines the minimum wall thickness required to avoid out-of-plane instability, given an unsupported wall height between points of lateral support (usually in the form of floor and roof diaphragms). The minimum required thickness depends on several parameters, including the longitudinal reinforcement ratio, curvature and displacement ductility demands over the plastic hinge, plastic hinge height, aspect ratio (height/length) and the respective mechanical properties of the steel and masonry

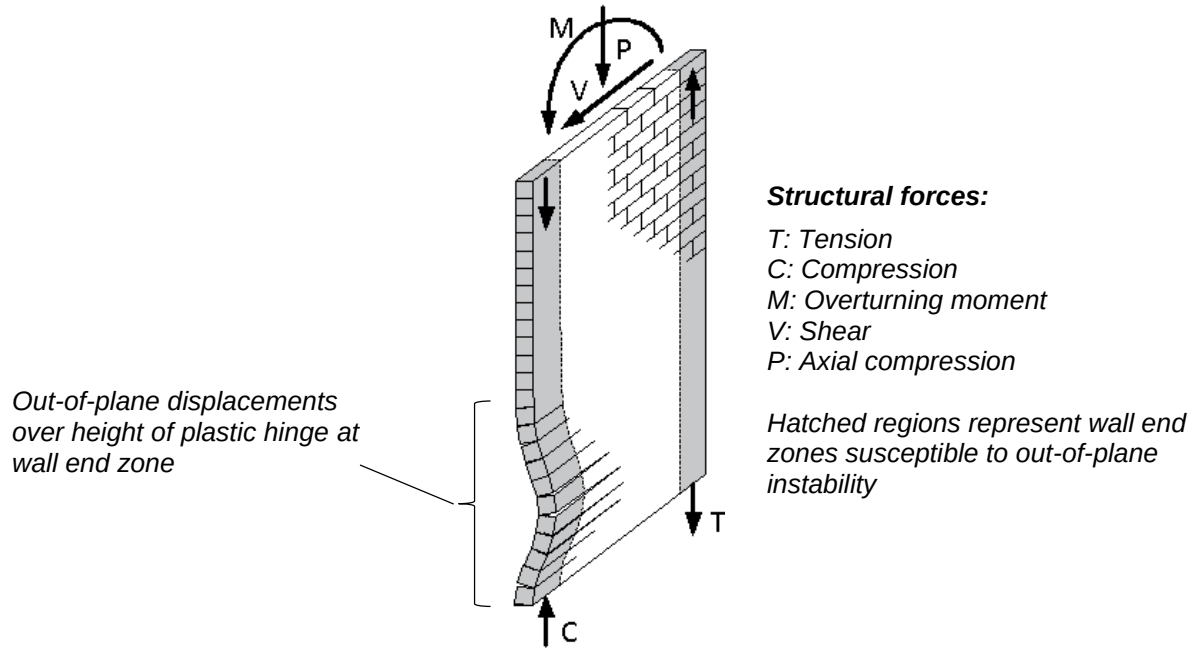

materials.

Fig. 1 – Out-of-plane instability of a RMSW subjected to in-plane loading

However, a nearly complete lack of experimental evidence related to the out-of-plane stability of RMSWs exists and therefore the h/t limits set by CSA S304-14 have not been experimentally verified. This lack of evidence prompted the need for the ongoing comprehensive research program focused on establishing rational criteria for the prevention of this undesirable mechanism. Phase 1 of the program included an experimental study on five full-scale slender reinforced masonry prismatic specimens subjected to uniaxial reversed cyclic loading. The specimen cross-section and reinforcement were designed to model the end zones of a laterally loaded RMSW with an h/t ratio of 27 - significantly higher than the CSA S304-14 h/t limit of 16 for Ductile Shear Wall class (Azimikor, 2012a, 2012b). The primary objective of these tests was to observe and better understand the instability phenomenon in RMSWs. Moreover, the tests were also conducted as a preliminary investigation into the magnitude of tensile strain required to precipitate out-of-plane instability of a RMSW end zone, while neglecting the vertical and lateral strain gradient effects characteristic of a full-scale RMSW.

Phase 2 of the research program, currently in progress, utilized the results of Phase 1 to design five full-scale slender RMSW specimens with h/t ratios ranging from 21 to 29. The specimens had different aspect ratios, vertical and horizontal reinforcement ratios and detailing, and applied axial compressive stress level (Robazza 2013a, 2013b, 2015). The specimens were instrumented to record out-of-plane displacements and analyze the lateral stability of the specimens throughout the test. The initial results of the research have indicated that the current h/t limits are not only overly conservative for slender RMSWs, but also that h/t limits alone may not provide adequate criteria for the evaluation of lateral stability. Lateral stability of slender

RMSWs is found to be very complex and its development depends on many factors including typical wall design parameters and the prior occurrence of other prevalent RMSW failure mechanisms. This paper outlines the experimental program and the key findings of Phase 2 to date.

2. Experimental Program

2.1. Wall Design and Construction

Professional masons constructed the five full-scale RMSW specimens at the UBC Structures Laboratory. The tests were planned with the intention to induce an out-of-plane instability failure mechanism in the specimens. All specimens were fully grouted and reinforced with horizontal and vertical reinforcement while adhering to the CSA S304-14 ductile detailing requirements. The following parameters related to dimensions and construction practice were varied to create the test matrix summarized in Table 1: amount, layout, and detailing of vertical and horizontal reinforcement, as well as the wall h/t and aspect ratios. Furthermore, the applied axial stress level and the test setup were also varied.

Table 1 – Wall specimen test matrix

Wall ID	Lateral Support Type	Wall Design Parameters								Varied Parameter
		h (mm)	t (mm)	L (mm)	ρ_v (%)	ρ_h (%)	h/t --	h/L --	Axial Stress --	
W1	1	3800	140	2600	0.33	0.36	27.1	1.5	$0.03f'_m$	*Axial stress*
W2	1	3800	140	2600	0.33	0.36	27.1	1.5	0	*Reference case*
W3	2	4000	190	2600	0.24	0.26	21.1	1.5	0	*Thickness / Reinf. layout*
W4	2	4000	190	1400	0.15	0.26	21.1	2.9	0	*H/L aspect ratio*
W5	2	4000	140	2600	0.33	0.36	28.6	1.5	0	*Lateral support type*

The masonry units were laid in running bond using Type S mortar for the face shell bedding and consisted of standard Canadian hollow concrete blocks (390 mm length x 190 mm height) with either 140 or 190 mm thickness (**t**), thereby resulting in different **h/t** ratios. The specimen height was constrained by the height of the testing setup, but the length (**L**) was varied to ensure the formation of a plastic hinge at the base of the wall during testing, a prerequisite for the out-of-plane instability mechanism. Vertical reinforcement consisted of 10M and 15M deformed steel bars which were continuous over the full wall height (no lap splices) and fully developed in heavily reinforced concrete footings using 180° hooks. The horizontal reinforcing bars were placed in bond beam blocks and were continuous between 180° end hooks. The vertical reinforcement ratio (ρ_v) varied from 0.15 to 0.33% (the latter value was considered typical for Canadian masonry construction practice) whereas the horizontal reinforcement ratio (ρ_h) varied from 0.26 to 0.36% (higher than typical for Canadian design practice). The objective was to induce a flexural failure mode and prevent significant shear deformations. The specimens were fully grouted with a commercially available coarse grout mix, which was poured in two half-height lifts for specimens W1 and W2 and a single lift for the remaining specimens. Masonry and steel material properties were reported by Robazza (Robazza, 2013b, 2013c).

2.2. Test Setup

The test setups used for the testing comprised of a rigid reinforced concrete reaction wall and floor, and either one or three hydraulic actuators, as shown in Figures 2 and 3. The actuator capacities were ±1000 kN for Actuator 1 and ±645 kN for Actuators 2 and 3. All three actuators were utilized for the first test (specimen W1) as shown in Fig. 3a; however only Actuator 1 was utilized for the remaining tests, as shown in Fig. 3b. Two different customized lateral supports (labelled as Type 1 and 2 in Table 1 and depicted in Fig. 3a and 3b respectively) were incorporated during the testing to prevent out-of-plane displacements at

the top of the wall (the latter support type was considered an improvement). Instrumentation of the test specimens is described by Robazza (Robazza, 2013b, 2013c).

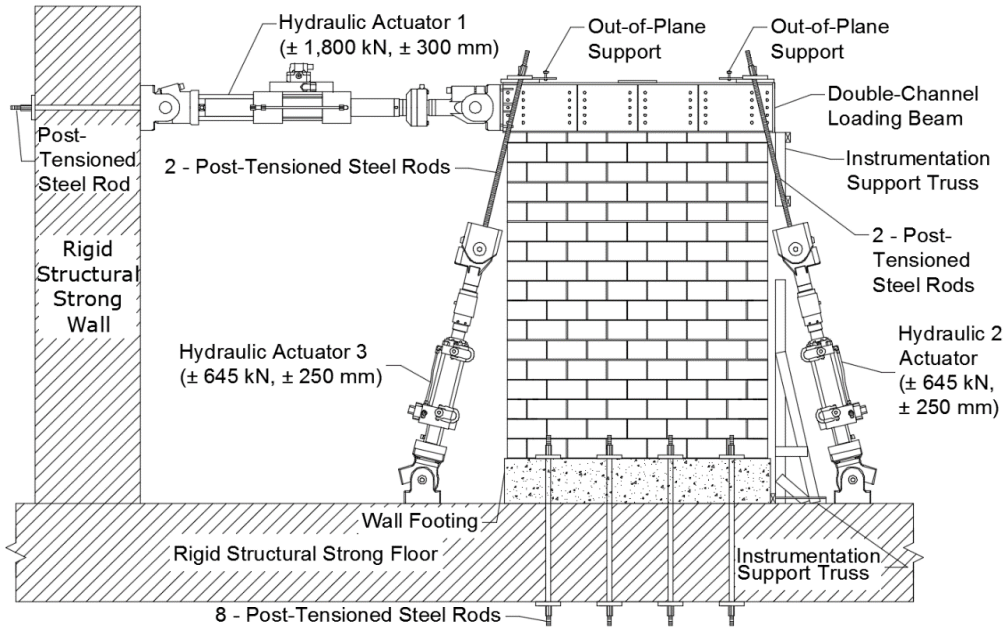

Fig. 2 – Test setup at the UBC Structures Laboratory: key components

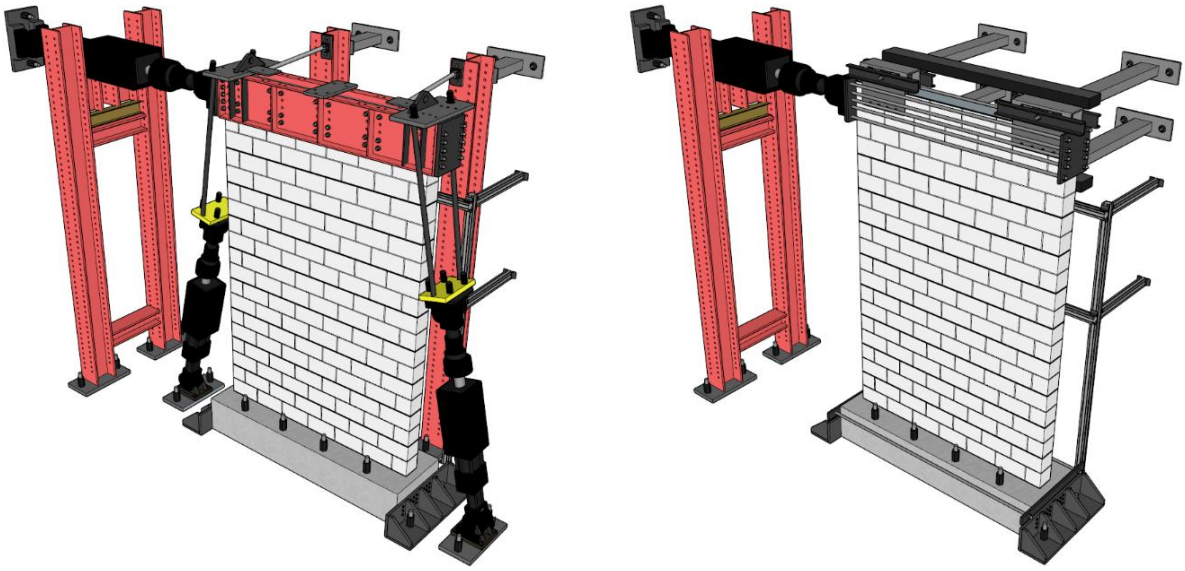

a) **b)**

Fig. 3 – Test setups: a) specimen W1, and b) specimens W2-W5

2.3. Loading Protocol

The specimens were subjected to the reversed cyclic loading protocol shown in Fig. 4. Lateral in-plane loading was applied by Actuator 1. For specimen W1, an initial vertical compression load of 330 kN was applied by Actuators 2 and 3. The loads applied by Actuators 2 and 3 were varied during the test to simulate the effect of overturning moment on the bottom storey of a multi-storey building but in a way such that a constant simulated gravity load was consistently maintained. The loading protocol was displacement-controlled, and consisted of one or more cycles of a predetermined lateral displacement. The cyclic displacements were incrementally increased until the lateral load-carrying capacity was completely exhausted. The target displacement for each cycle was expressed in terms of Δ_y, that is, the displacement

corresponding to yielding of the outermost longitudinal reinforcing bars at the wall ends. The Δ_y value of 7 mm was determined by analysis and confirmed by the test data collected from specimen W1. This displacement increment was utilized for all subsequent tests for consistency.

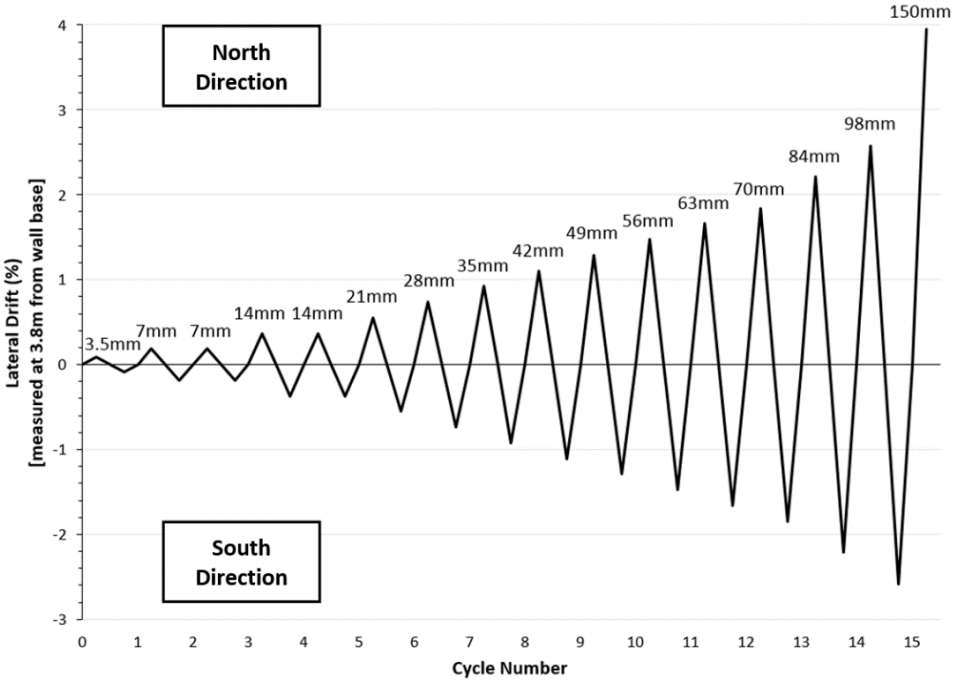

Fig. 4 – Lateral loading protocol

3. Experimental Results: Specimen Behaviour and Damage Observations

3.1. General Damage Patterns and Failure Mechanisms

The behaviour of all specimens was dominated by a flexural response, as evidenced by significant cracking at horizontal bed joints that was initiated at the wall end zones and which extended over the height of the plastic hinge. The cracking was observed at low drift levels and it rapidly progressed from the wall base up the wall height. At higher drift levels, the horizontal cracks were accompanied by comparatively small diagonal shear cracks that usually propagated from the horizontal cracks at the wall ends. These cracks generally followed a step-like pattern along the mortar joints and propagated toward the wall mid-length during successive loading cycles. Eventually, during the final stages of testing, these inclined cracks occasionally propagated through the block face shells at the wall end zones.

Small sliding displacements (approximately 1-2 mm) were observed after several cycles of loading beyond yield in the specimens without applied compressive stress. These displacements showed a tendency to continually increase, and they accounted for approximately 20% of the total drift at drift levels of approximately 1.1 to 1.5%. This ratio of sliding to total drift would generally remain between 20 to 30% for most specimens as the combined effects of dowel action support and toe crushing would eventually stabilize their propagation. The primary sliding crack usually developed at the wall base, although generally much smaller amounts of sliding occasionally occurred at the second or third course as well, depending on the horizontal reinforcement layout.

At drift levels between 1.3 and 1.6%, vertical splitting cracks began to appear at the compression toes due to large curvatures developing over the specimen plastic hinge height. These cracks extended through the bottom 2 or 3 courses during subsequent loading cycles (see Fig. 5a). Even a small amount of applied axial compression caused a substantial decrease in the drift corresponding to this type of damage (e.g. the case of specimen W1). Subsequently, inclined cracks forming through the face shells at the compression toe severely compromised the integrity of those face shells. As the vertical reinforcing bars within these face shells were compressed after being elongated in the previous cycle, the bars would deform out-out-of-plane, thereby contributing to face shell spalling soon after load reversal. In addition, wide horizontal bed

joint cracks, clearly visible at the tension end zone, also contributed to spalling of the face shells. Ultimately, the face shells would debond from the grouted cores, which remained largely intact, except for minor vertical cracks occurring on both sides of the wall at the location of the vertical reinforcing bar within the grouted core (see Fig. 5b). Spalling of the face shells and cracking of the grouted cores became more significant at higher drift levels. Eventually, crushing of the grouted cores took place, thereby exposing the vertical reinforcing bars at the wall end zones (see Fig. 5c). Some of these exposed bars buckled when the end zone was in compression, and straightened when the end zone reversed into tension. This further contributed to spalling of the grouted cores as the buckling bars had a tendency to push away the surrounding grout. During subsequent load cycles, these damage patterns extended from the wall end zones toward the wall's mid-length, following the shift of the effective compression zone (see Fig.s 5d and 5e). For most of the specimens, subsequent load cycles caused further disintegration of the remaining face shells and grouted cores over the bottom courses and the wall would eventually collapse out-of-plane.

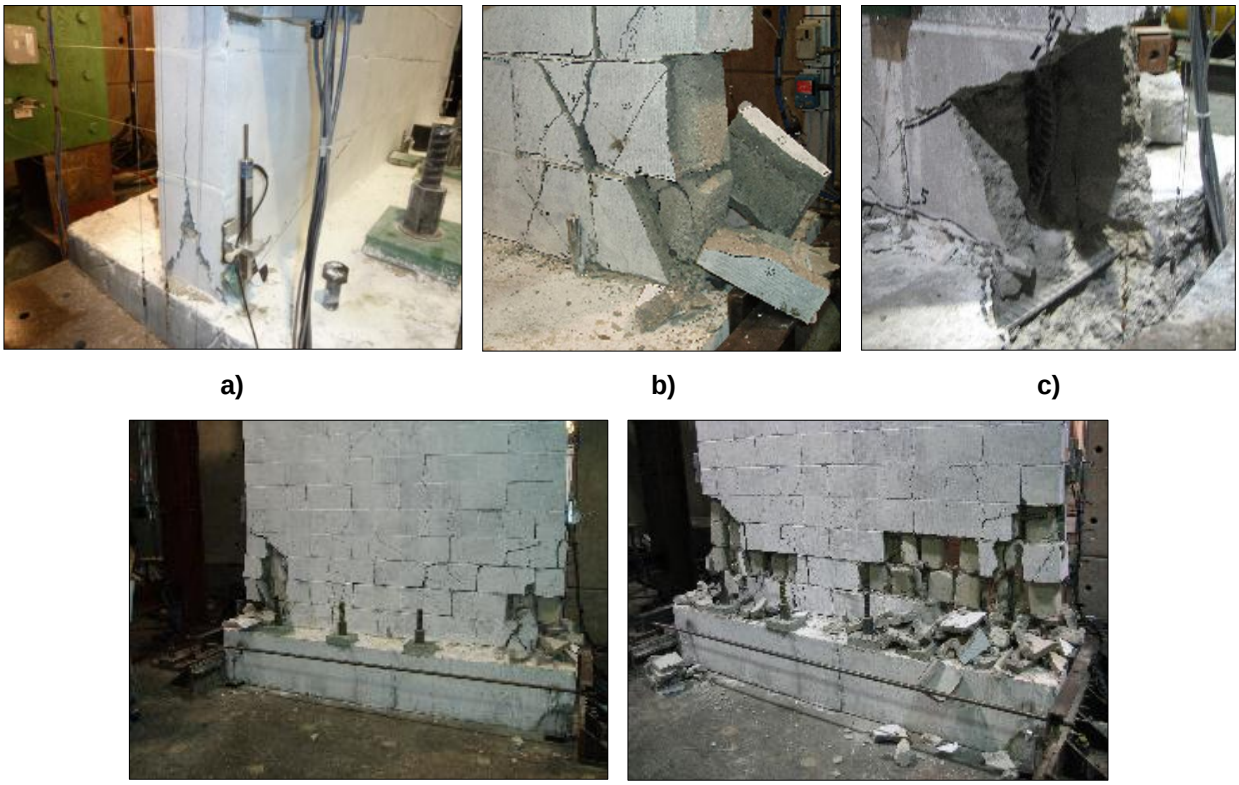

a) **b)** **c)**

d) **e)**

Fig. 5 – Typical damage patterns in various wall specimens: a) face shell splitting at wall toe; b) face shell spalling; c) exposed rebar buckling after crushing and spalling; d) and e) damage progression from the toes toward middle portion of the wall

3.2. Load-Displacement Relationships

Key values from the lateral load-displacement hysteresis envelopes are presented in Table 2 based on the backbone envelope points defined in Fig. 6. The complete lateral load-displacement hystereses are provided in Fig 7. As all plots are shown using the same scale, the contrasting behaviour among the specimens is readily apparent. The effect of axial compressive stress is notable when comparing the response of specimen W1 (see Fig. 7a), which had an axial stress of $0.034f'_m$, to the other four specimens which did not have any applied axial stress. The axial compressive stress resulted in an increase in shear and flexural strength, but it also caused a rapid strength degradation after the ultimate load capacity had been attained. Furthermore, axial stress limited the extent of sliding shear at the base of the wall and is evidenced by the pinching behaviour in all hysteresis curves (except for specimen W1).

The influence of the amount of vertical reinforcement is apparent in the hysteretic behaviour of specimen W4, which was characterized by the highest aspect ratio (2.9) of all the specimens. Despite having a higher aspect ratio, the inelastic deformation was concentrated at the wall base in the form of rocking and sliding after the yielding of the vertical reinforcement took place. The lateral load-resisting capacity of W4 was significantly lower compared to other specimens due to its significantly lower vertical reinforcement ratio (by 38 to 65%). The aspect ratio appeared to have played a comparatively minor role related to the overall specimen behaviour, besides decreasing the elastic stiffness of specimen W4 relative to the other specimens (see Fig. 7d).

Specimens W2 and W3 had an equal area of vertical reinforcement, however specimen W3 had a 36% larger wall thickness, and thus the vertical reinforcement ratio was 27% lower than W2. As both specimens were designed to exhibit ductile flexural behaviour, the ultimate strengths of the two specimens were within 5% of each other. Larger wall thickness might have contributed to increased stability of W3 and slower strength degradation after face shell spalling. This was demonstrated by the significantly higher displacement ductility ratio attained by W3 as compared to W2 (see Fig.'s 7b and 7c).

The incomplete grouting at the toes of specimen W5 became apparent immediately after yielding of the vertical reinforcement when wide flexural cracks formed at the wall toe. These cracks subsequently led to premature and rapid face shell spalling and toe crushing, thereby greatly reducing the displacement ductility capacity of the specimen (see Fig. 7e). It should be noted that specimens W2 and W5 had identical designs, except for a change in the lateral support for the test setup, which was deemed not to influence the behaviour.

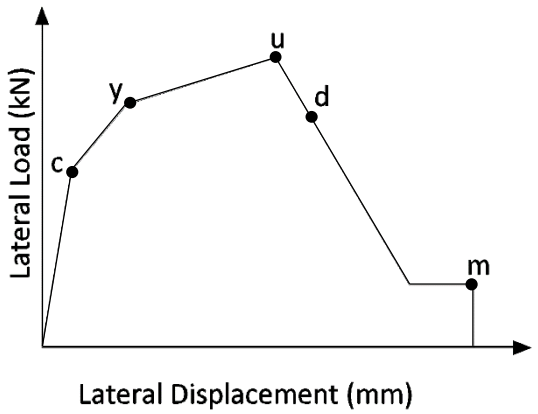

Structural behaviour at specified backbone points:

c: First cracking
y: First yielding of vertical reinforcement
u: Ultimate load capacity
d: 80% of ultimate load capacity
m: Maximum displacement ductility

Fig. 6 – Backbone envelope based on lateral load-displacement hystereses of Fig. 6

Table 2 – Comparison of lateral load - displacement hystereses

Wall ID	Direction	Lateral Load (kN)					Lateral Drift (mm/mm)				
		Q_c	Q_y	Q_u	Q_d	Q_m	D_c	D_y	D_u	D_d	D_m
W1	1	124	199	250	200	174	0.10	0.23	0.38	0.56	0.84
	2	126	184	249	200	149	0.09	0.23	0.49	0.69	0.72
W2	1	99	185	217	174	155	0.09	0.34	1.27	1.82	2.56
	2	74	170	199	160	123	0.07	0.29	0.66	1.43	2.15
W3	1	109	155	206	164	138	0.05	0.11	0.60	2.08	3.96
	2	96	132	183	146	139	0.09	0.20	1.26	2.23	2.59
W4	1	20	35	43	35	38	0.07	0.14	1.03	1.84	2.15
	2	17	27	34	27	2	0.06	0.08	1.31	1.23	1.88
W5	1	111	187	188	150	75	0.03	0.18	0.19	0.54	1.62
	2	92	159	181	145	6	0.12	0.39	0.74	1.28	1.88

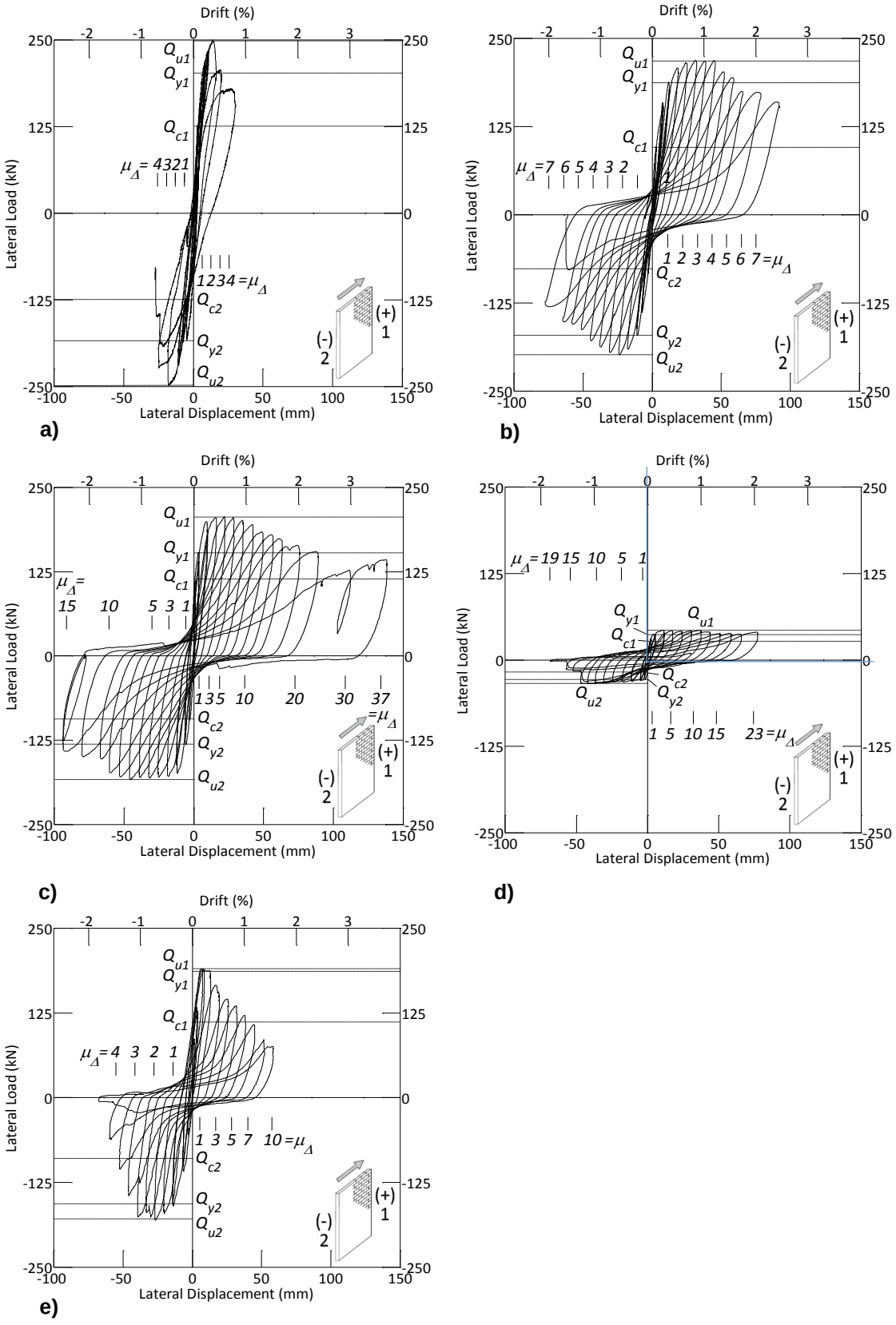

Fig. 7 – Lateral load-displacement behaviour of specimens: a) W1, b) W2, c) W3, d) W4, and e) W5

3.3. Out-of-Plane Instability Failure Mechanism

Out-of-plane displacements at the wall end zones were well controlled (less than 20 mm) throughout all of the tests except for the test on specimen W2. In the case of the test on W2, out-of-plane displacements were initiated relatively early on in the test (0.55% drift) and continued to increase during subsequent cycles. Eventually these out-of-plane displacements resulted in wall instability after increasing to a value of over half of the wall thickness. The observed out-of-plane instability failure mechanism with Fig. 8.

When a wall end zone is subjected to relatively high tensile strains (point **1**), fairly uniform tensile cracking develops along the mortar joints over the plastic hinge height. During load reversal (point **2**), increasing compression stresses in the wall end zone are resisted solely by the vertical reinforcing bars extending across the open horizontal cracks. This may cause the end zone to displace out-of-plane due to eccentric bar placement and/or load path, even at very low compression stress levels. At this stage, two mechanisms of response with different consequences are possible (denoted with points **3a** and **3b**). The first mechanism (point **3a**) develops when the flexural cracks close before out-of-plane displacements attain a critical value (theoretically half of the wall thickness). A restoring bending moment develops due to internal compressive forces in the masonry face shells, assuming they have not spalled at this stage. This causes the lateral stiffness of the end zone to be restored and brings it back to a nearly plumb position (point **4**); however, some residual displacements may remain due to misalignments between masonry units as the cracks had closed while the end zone was still displaced out-of-plane. The second mechanism (point **3b**) develops when the flexural cracks do not close prior to the critical out-of-plane displacement being attained. In this case, the out-of-plane displacements will continue to increase and out-of-plane instability will ensue.

If out-of-plane instability does not take place (point **3a**) and the specimen's vertical alignment is restored (point **4**), out-of-plane displacements may increase by a small amount due to elastic compressive strain recovery in the vertical reinforcing bars which deformed eccentrically during the initial crack closure (point **5**). However, these displacements are expected to steadily decline as the end zone is subjected to high tensile stresses (point **6**), and eventually drop to approximately zero value when the end zone specimen returns to the original position in tension (point **1**).

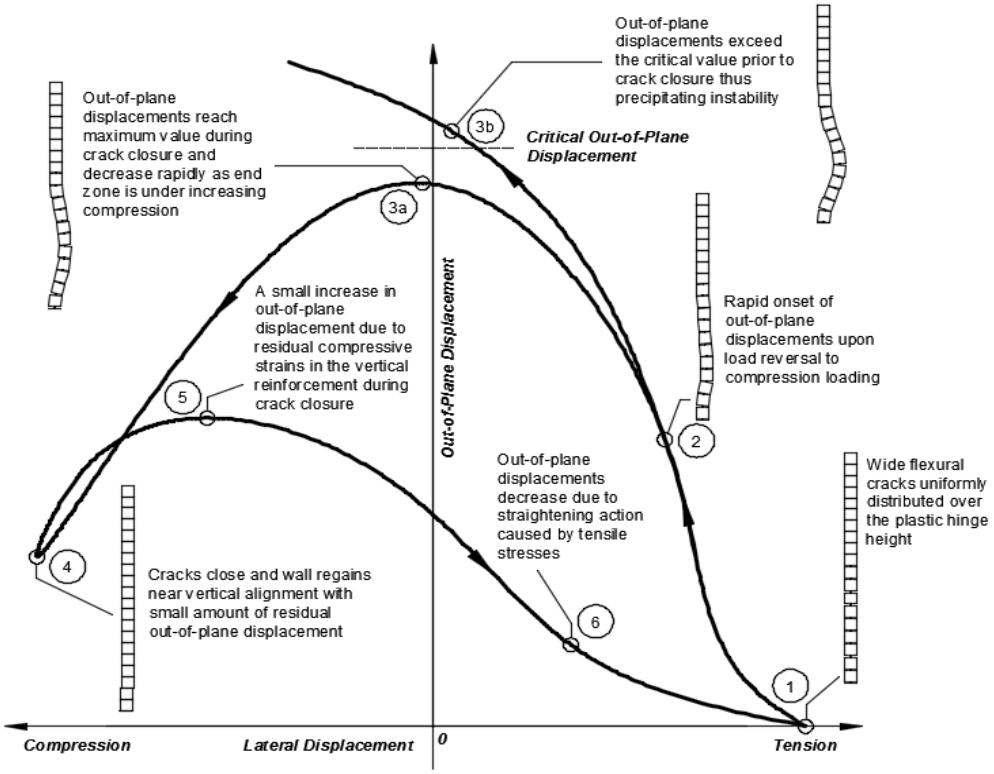

Fig. 8 – A cycle of out-of-plane versus lateral in-plane displacements in a wall subjected to in-plane reversed cyclic loading (recorded at half of the end zone plastic hinge height)

4. Key Observations and Conclusions

The following key observations and conclusions were developed based on the quantitative and qualitative data provided by the experimental testing phases of this research program to date:

1. **Effect of h/t ratio**: Although all specimens were designed with h/t ratios that were between 50 to 105% greater than the current CSA S304-14 limits, only specimen W2 experienced out-of-plane displacements leading to instability. Despite the limited number of tests conducted thus far, the current h/t limits appear conservative. Further experimental evidence is required to confirm this conclusion and it is expected that the next test series may provide such evidence

2. **Influence of other failure mechanisms**: Other prevalent RMSW failure mechanisms appeared to often govern the response of the specimens and prevent the development of the out-of-plane instability failure mechanism. Flexural toe crushing and face shell spalling prior to the advance of high axial tensile strains over the plastic hinge height at the wall end zone would prevent these strains from developing uniformly, and instead concentrate them at the crushed and spalled courses, drastically decreasing the probability of global instability. Sliding shear displacements at the wall base also precluded out-of-plane instability by engaging dowel action of the vertical reinforcement, encouraging these bars to deform in-plane versus out-of-plane upon load reversal. Future investigation will be aimed at relating drift limits to each RMSW failure mechanism.

3. **Effect of strain gradient**: Strain gradient effects over both the wall height and length were observed to significantly increase the resistance toward out-of-plane displacements. The vast majority of experimental tests supporting the current theoretical out-of-plane stability models have been conducted on uniaxial specimens in which strain gradient effects were neglected. Quantification of the strain gradient effects will be conducted in the next program phases.

4. **Unsupported height**: Current out-of-plane stability models utilize a theoretical plastic hinge height as the key parameter in defining the height of the wall that will be subjected to out-of-plane displacements. Observing the differences in cracking uniformity over the height of the specimens demonstrated that the unsupported height is indeed very important. Future phases of the program will thus be aimed at developing stability criteria which incorporate this parameter as a variable.

5. Acknowledgements

The project was generously sponsored by the Natural Sciences and Engineering Research Council of Canada (NSERC) under the Collaborative Research and Development Program, the Canadian Concrete Masonry Producers Association, and the Masonry Institute of British Columbia. The first author acknowledges the support provided by the NSERC Industrial Postgraduate Scholarship program. Wall reinforcement was graciously donated by Harris Rebar Ltd and Heritage Rebar Ltd.

6. References

Azimikor, Nazli, “Out-of-Plane Stability of Reinforced Masonry Shear Walls under Seismic Loading: Cyclic Uniaxial Tests”, *Master’s Thesis, University of British Columbia,* 2012a.

Azimikor, Nazli, Robazza, Brook R., Elwood, Kenneth J., Anderson, Donald L., Brzev, Svetlana, “An Experimental Study on the Out-of-Plane Stability of Reinforced Masonry Shear Walls”, *15th World Conference of Earthquake Engineering,* 2012b.

Canadian Standards Association, “CSA S304-14, Masonry Design of Buildings”, 2014.

National Research Council of Canada, “National Building Code of Canada”, 2010.

Paulay, Thomas, Priestley, Nigel M.J., “Stability of Ductile Structural Walls”, *Structural Journal, American Concrete Institute,* 90(1), 1993, pp. 385-392.

Robazza, Brook R., Brzev, Svetlana, Elwood, Kenneth J., Anderson, Donald L. Yang, Tony Y., “A Study on the Out-Of-Plane Stability of Ductile Reinforced Masonry Shear Walls Subjected To In-Plane Reversed Cyclic Loading”, *12th North American Masonry Conference,* 2015.

Robazza, Brook R., “Out-of-Plane Stability of Reinforced Masonry Shear Walls under Seismic Loading: In-Plane Reversed Cyclic Testing”, *Master’s Thesis University of British Columbia,* 2013a.

Robazza, Brook R., Elwood, Kenneth J., Anderson, Donald L., Brzev, Svetlana, “In-Plane Seismic Behaviour of Slender Reinforced Masonry Shear Walls: Experimental Results”, *12th Canadian Masonry Symposium,* 2013b.